scientific reports

Check for updates

OPEN

Bifurcation analysis and soliton solutions of the generalized third-order nonlinear Schrödinger equation using two analytical approaches

Shahida Parveen[1], Muhammad Abbas[1]✉, Tahir Nazir[1], Muhammad Nadeem Anwar[2], M. R. Alharthi[3], Muhammad Zain Yousaf[1] & Asnake Birhanu[4]✉

This research paper is used to examine the generalized third-order nonlinear Schrödinger equation that is important for the description of complex nonlinear wave propagation in optical fibers, plasma physics, and in fluid mechanics. By using the generalized auxiliary equation method and improved modified Sardar-sub equation method various analytical soliton solutions are obtained. The Periodic, bell, anti-bell, dark, W-type, kink, anti-kink, and M-shape solitons solutions of the problem are obtained by using proposed methods. The behavior of several soliton solutions is depicted graphically. The findings are important for applications in engineering and mathematical physics. A key component of planar dynamical system theory is the bifurcation of the dynamical system of the governing equation caused by the Galilean transformation. By emphasizing how susceptible the system is to its initial conditions and how uncertain its long-term evolution is, the study also investigates chaotic behavior. Lastly, sensitivity analysis is performed to examine the effects of altering system parameters on the stability and results of the solutions. By taking these things into account, this work aids in our comprehension of the proposed model's dynamical characteristics and offers helpful insights into its use in nonlinear media and other fields of research. In contrast to previous research, this work is novel because it applies enhanced analytical methods to the generalized third-order nonlinear Schrödinger equation, resulting in a wider range of solution classes.

Keywords Generalized third-order nonlinear Schrödinger equation, Generalized auxiliary equation method, Improved modified Sardar-sub equation method, Solitary wave solution, Bifurcation analysis

In real life, most systems are dynamic and nonlinear. If time is continuously varying, then the mathematical model to be developed is a Nonlinear partial differential equation (NLPDE). NLPDEs have been applied in numerous fields such as: fluids dynamics, biophysics, electromagnetic theory, plasma physics, electrochemistry, high energy physics, optical fibers, quantum mechanics and even in quantum field theories. The research in nonlinear equations is an interesting and important discipline that provides comprehensive data on solitary waves' dynamics in physical systems. Stable and localized wave solutions are the groundwork to research nonlinear models. One of the most sought-after models for describing soliton dynamics under varied circumstances are the complex Ginzburg–Landu equation[1], the (2+1)-dimensional complex modified Korteweg–de Vries system[2], Chen–Lee–Liu (pCLL) dynamical equation[3], Complex-Coupled Kuralay System (CCKS)[4], The Nonlinear Dispersive Modified Benjamin-Bona-Mahony Equation[5], cold bosonic atoms[6], the nonlinear Tzitaeica–Dodd–Bullough model[7], the nonlinear Pochhammer–Chree equation[8], the -dimensional generalized Burgers–Fisher (GBF) model[9], the fractional Chaffee-Infante equation[10] and (2 + 1)-dimensional Bogoyavlenskii's breaking soliton system[11], double dispersive sharma-Tasso-Olver equation[12], the Westervelt equation[13]. Some of the powerful and efficient methods for producing traveling wave solutions in various formats are the modified

[1]Department of Mathematics, University of Sargodha, Sargodha 40100, Pakistan. [2]Institute of Education, University of Sargodha, Sargodha 40100, Pakistan. [3]Department of Mathematics and Statistics, College of Science, Taif University, P.O.Box 11099, Taif 21944, Saudi Arabia. [4]Department of Mathematics,College of Science, Hawassa University, Hawassa, Ethiopia. ✉email: muhammad.abbas@uos.edu.pk; asnakeb@hu.edu.et

F-expansion approach[14], the nano-ionic currents equation[15], Hartree equation[16], the unconditionally stable (US) Chebyshev (CS) finite-difference time-domain (FDTD) method[17], nonlinear integral impulsive differential equation[18], the Bernoulli Sub-ODE method[19], Shynaray-IIA equations[20], the Kudryashov method[21] and the Sardar-sub equation method[22].

The generalized third-order nonlinear Schrödinger equation (NLSE), which includes higher-order terms and more intricate interactions, is the subject of this investigation. These higher order terms are important for better understanding and accurate modeling of the behavior of high-order waves. The generalized third-order nonlinear Schrödinger (NLSE) model models ultrashort optical pulse propagation in plasma systems and nonlinear fibers with higher-order effects such as self-steepening and third-order dispersion. These effects have not been fully investigated in earlier studies on their impact on soliton dynamics. This contribution bridges the gap by using the generalized auxiliary equation method and IMSSEM to derive new soliton solutions and examine the dynamical behavior. Here, the goal is to acquire exact solutions and examine how the solutions vary under different conditions using the generalized auxiliary aquation method and IMSSEM.

The motivation for using both methods lies in their complementary strengths. The generalized auxiliary aquation method provides a systematic and relatively simple framework for constructing a wide range of analytical solutions, while the IMSSEM extends this capability by introducing improved transformations and additional parameters that allow for more complex, generalized, and flexible soliton structures. The combined use of these two approaches not only ensures cross-validation of the obtained results but also enhances the diversity, accuracy, and physical interpretability of the solutions. Compared to traditional single-method approaches, the proposed combination offers broader solution sets and deeper insights into the nonlinear dynamics of the model. The originality of this work lies not only in the derivation of new classes of soliton and periodic wave solutions but also in performing a comprehensive dynamical analysis involving bifurcation, chaotic, and sensitivity studies. These findings reveal more about the intricate behavior of nonlinear systems and show how innovative and successful the suggested strategies are in comparison to other techniques. In the fields where higher-order effects are crucial for wave motion and behavior, such as optics, fluid dynamics and plasma physics, this approach will improve the analysis of rich wave behaviors and open up new possibilities for the use of nonlinear Schrödinger models. This work is novel in that it applies two potent analytical techniques to the generalized third-order NLS equation, which has not been thoroughly examined in prior research: the generalized auxiliary equation method and the IMSSEM. The combined dynamical analysis of bifurcation, chaos, and sensitivity was frequently overlooked in earlier works, which mainly concentrated on obtaining specific types of soliton solutions using traditional analytical techniques. As an alternative, the current study not only offers a more extensive and generalized class of analytical soliton solutions, but it also conducts a thorough dynamical analysis that includes sensitivity, bifurcation, and chaotic analyses to look at the model's stability and qualitative behavior. By providing more varied solution structures, enhanced analytical flexibility, and more profound physical insights into the nonlinear dynamics, this dual-method framework closes the gap in the literature and broadens the focus of earlier studies on the NLS equation.

Governing equation

The form of the generalized third-order NLSE is as follows[23]:

$$i\left(\frac{\partial w}{\partial t}+\frac{\partial^3 w}{\partial x^3}\right)+|w|^2\left(\beta_1 w+i\beta_2\frac{\partial w}{\partial x}\right)+i\beta_3\frac{\partial\left(|w|^2\right)}{\partial x^2}w=0. \tag{1.1}$$

The complex-valued function $w(x, t)$ and the values of the parameters β_1, β_2, and β_3 are all real numbers. Equation (1.1) is used to represent ultrashort pulses in optical fibers. In the equation above, the term of second order derivative appears usually. Third-order dispersion, which is represented by the third-order term in the generalized nonlinear Schrödinger equation, is crucial in optical fibers when ultrashort or broadband pulses are involved. It takes into consideration the frequency dependence of group velocity, which results in dispersive wave generation, self-steepening, and asymmetric pulse distortion. In contemporary high-speed or photonic crystal fibers, where higher-order dispersion greatly affects pulse shape and stability, the standard NLSE is unable to adequately characterize pulse propagation without this term. Nevertheless, after introducing the third order derivative expression, we are able to eliminate the second order derivative through a gauge transformation. When both $\beta_1 = \beta_3 = 0$, equation (1.1) turns out to be the complex version of the modified KdV or Hirota equation and is solved by the inverse scattering transform method. Nasreen et al.[24] used the generalized Riccati mapping approach to give a list of several types of soliton solutions to the model. The model in this study is founded on a deterministic approach that disregards stochastic perturbations or the effects of noise. For actual physical systems like optical fibers or plasmas, a random fluctuation can affect soliton amplitude and stability. Bifurcation analysis is the study of how changes in parameters or otherwise affect the qualitative changes in the solutions of a system[25,26]. Bifurcations may occur due to the loss of old solutions, or stability shifts. It is useful for deriving insights of such systems' behavior in real life applications and prediction and control of such systems' behavior. To determine if a dynamical system displays periodic solutions or chaotic behavior, then introduced a perturbed term into the resulting dynamical system. In physics, engineering, economics and communication chaotic behavior is exhibited. Moreover, the sensitivity analysis of the dynamical system also shows that minor adjustments to the initial conditions have no effect on the solution's stability[27].

In this research, generalized auxiliary equation method and IMSSEM are used to solve the generalized third-order NLSE. The various soliton solutions are obtained including M-shape solitons, bell, anti-bell, kink, anti-kink, periodic and dark solitons. Dynamical analysis of the proposed model are carried out by applying concepts from planar dynamical systems. Although exact solutions are already available, the same kind of solutions derived

through other analytical methods serve to validate, generalize, and compare the efficiency. The same physical behavior can be shown by each method via a different mathematical path, verifying the correctness and stability of the earlier known results. Additionally, certain methods such as generalized auxiliary equation method and IMSSEM can yield simpler expressions, wider ranges of parameters, or new families of solutions, thereby further extending the understanding and range of applicability of the model.. This research provides important insights into the transitions between stable, unstable or chaotic states by closely analyzing the qualitative changes in a system's behavior brought about by parameter adjustments. Sensitivity analysis can also be used to determine how the dynamics of the system behave when parameters are changed.

This paper organized as follows: In section 2, the generalized third-order NLSE is introduced, along with its formulation and significance in the theory of nonlinear waves. In section 3, the generalized auxiliary equation method and IMSSEM are given. Moving on to section 4, the article discusses the applications of these two methods. Visual evaluations and physical interpretation are discussed in section 5 and section 6, respectively. In section 7, the dynamical analysis of the proposed model is discussed. In section 8, novelty and comparison is discussed. In section 9, the conclusion is given.

Wave transformation

The model (1.1) is solved by choosing the following hypothesis.

$$w(x,t) = \phi(\xi)e^{iQ(x,t)}, \tag{2.1}$$

where $\xi = sx + pt$ and $Q(x,t) = \alpha x + \gamma t + \theta$. In the wave profile, the amplitude component is represented as ϕ and Q shows the phase factor. The frequencies of soliton are denoted by s and α. The wave numbers are denoted by p and γ, while the phase constant is θ. Equation (2.1) is substituted into equation (1.1), the real and imaginary parts are separated to obtain

$$3\alpha s^2\phi'' + (\gamma - \alpha^3)\phi + (\beta_2\alpha - \beta_1)\phi^3 = 0. \tag{2.2}$$

$$s^3\phi^{(3)} + (p - 3\alpha^2 s)\phi' + s(\beta_2 + 2\beta_3)\phi^2\phi' = 0. \tag{2.3}$$

Equation (2.3) is integrated and the integration constant is set to zero. Then

$$s^3\phi'' + (p - 3\alpha^2 s)\phi + \frac{s}{3}(\beta_2 + 2\beta_3)\phi^3 = 0. \tag{2.4}$$

Due to the similarities between equations (2.2) and (2.4), the coefficients have the following relationship: $\beta_1 = -2\beta_3\alpha, \gamma = \frac{3\alpha p - 8\alpha^3 s}{s}$

Methodologies

Generalized auxiliary equation method

To determine the exact solitory wave solutions of NLPDEs, the generalized auxiliary equation approach is employed[28]. The primary steps are listed below.

Step-1 The following is the standard form of NLPDE:

$$S(\psi, \frac{\partial\psi}{\partial x}, \frac{\partial\psi}{\partial t}, \dots) = 0, \tag{3.1}$$

Applying the transformation

$$\psi(x,t) = N(\xi), \xi(x,t) = sx + pt. \tag{3.2}$$

By substituting equation (3.2) into equation (3.1), the NLODE is obtained as:

$$O(N, N', N'', \dots) = 0. \tag{3.3}$$

Step-2 Assuming that equation (3.3) has a solution

$$N(\xi) = a_0 + \sum_{i=1}^{J} a_i\varpi^i(\xi), a_N \neq 0, \tag{3.4}$$

where the constants $a_i (i = 1, 2, 3, \dots, J)$ are to be found thereafter. The following auxiliary equation is satisfied by the function $\zeta'(\xi)$:

$$\varpi'(\xi) = \sqrt{q_1\varpi(\xi)^2 + q_2\varpi(\xi)^3 + q_3\varpi(\xi)^4}. \tag{3.5}$$

Step-3 The balancing strategy for the value of J will be applied in this step.

Step-4 Inserting equation (3.4) with equation (3.5) into equation (3.3). The family of solutions of equation (3.1) is thus obtained.

Trigonometric hyperbolic solutions

$$\varpi(\xi) = \frac{-q_1 q_2 \text{sech}^2(\frac{\sqrt{q_1}}{2}\xi)}{q_2 - q_1 q_3(1 \pm \tanh(\frac{\sqrt{q_1}}{2}\xi)}, b_1 > 0. \tag{3.6}$$

$$\varpi(\xi) = \frac{q_1 q_2 \text{csch}^2(\frac{\sqrt{q_1}}{2}\xi)}{q_2 - q_1 q_3(1 \pm \coth(\frac{\sqrt{q_1}}{2}\xi)}, b_1 > 0. \tag{3.7}$$

$$\varpi(\xi) = \frac{2q_1 \text{sech}^2(\sqrt{q_1}\xi)}{\pm\sqrt{\zeta} - q_2 \text{sech}(\sqrt{q_1}\xi)}, q_1 > 0, \zeta > 0. \tag{3.8}$$

$$\varpi(\xi) = \frac{2q_1 \text{csch}^2(\sqrt{q_1}\xi)}{\pm\sqrt{-\zeta} - q_2 \text{sech}(\sqrt{q_1}\xi)}, q_1 > 0, \zeta > 0. \tag{3.9}$$

$$\varpi(\xi) = \frac{-q_1 \text{sech}^2(\frac{\sqrt{q_1}}{2}\xi)}{q_2 \pm 2\sqrt{q_1 q_3}\tanh(\frac{\sqrt{q_1}}{2}\xi)}, q_1 > 0, \zeta > 0. \tag{3.10}$$

$$\varpi(\xi) = \frac{q_1 \text{csch}^2(\frac{\sqrt{q_1}}{2}\xi)}{q_2 \pm 2\sqrt{q_1 q_3}\coth(\frac{\sqrt{q_1}}{2}\xi)}, q_1 > 0, \zeta > 0. \tag{3.11}$$

$$\varpi(\xi) = -\frac{q_1}{q_2}(1 \pm \tanh(\frac{\sqrt{q_1}}{2}\xi)), q_1 > 0, \zeta = 0. \tag{3.12}$$

$$\varpi(\xi) = -\frac{q_1}{q_2}(1 \pm \coth(\frac{\sqrt{q_1}}{2}\xi)), q_1 > 0, \zeta = 0. \tag{3.13}$$

Trigonometric solutions

$$\varpi(\xi) = \frac{-q_1 \sec^2(\frac{\sqrt{-q_1}}{2}\xi)}{q_2 - 2\sqrt{-q_1 q_3}(\tan(\frac{\sqrt{-q_1}}{2}\xi)}, q_1 > 0, \zeta > 0. \tag{3.14}$$

$$\varpi(\xi) = \frac{-q_1 \csc^2(\frac{\sqrt{-q_1}}{2}\xi)}{q_2 - 2\sqrt{-q_1 q_3}(\cot(\frac{\sqrt{-q_1}}{2}\xi)}, q_1 > 0, \zeta > 0. \tag{3.15}$$

$$\varpi(\xi) = \frac{2q_1 \sec^2(\sqrt{-q_1}\xi)}{\pm\zeta - b_2 \sec(\sqrt{-q_1}\xi)8}, q_1 > 0, \zeta > 0. \tag{3.16}$$

$$\varpi(\xi) = \frac{2q_1 \csc^2(\sqrt{-q_1}\xi)}{\pm\zeta - b_2 \sec(\sqrt{-q_1}\xi)8}, q_1 > 0, \zeta > 0. \tag{3.17}$$

Exponential solutions

$$\varpi(\xi) = \frac{4q_1 \exp^{\pm\sqrt{q_1}\xi}}{(\exp^{\pm\sqrt{q_1}\xi} - q_2)^2 - 4q_1 q_3}, q_1 > 0. \tag{3.18}$$

$$\varpi(\xi) = \frac{\pm 4q_1 \exp^{\pm\sqrt{q_1}\xi}}{1 - 4b_1 b_3 \exp^{\pm 2\sqrt{q_1}\xi}}, q_1 > 0, q_2 = 0. \tag{3.19}$$

Rational solutions

$$\varpi(\xi) = \frac{\pm q_1 q_2}{b_2^2 \varkappa^2 - q_1 q_3}, q_1 > 0. \tag{3.20}$$

$$\varpi(\xi) = \pm\frac{1}{\sqrt{q_3}\xi}, q_1 = 0, q_2 = 0, \tag{3.21}$$

where $\zeta = q_1^2 - 4q_1 q_3$.

Improved modified Sardar-sub equation method

$$O(M, M_t, M_x, M_{xx}, \dots). \tag{3.22}$$

To continue the research, in the context of the applied wave transformation, the function $M = M(x, t)$ denotes an unknown function. An overview of this wave transition is provided here:

$$M = M(\xi), \tag{3.23}$$

where $\xi = x - rt$. The PDE is transformed into an ODE of integer order by inserting equation (3.23) into equation (3.22).

$$O(M', M'', M''', \dots) = 0. \tag{3.24}$$

In equation (3.24), the ODE was solved using the IMSSEM. The standard form of the approach is as follows:

$$M(\xi) = a_0 + \sum_{j=1}^{P} a_j \phi^j(\xi), a_K \neq 0, \tag{3.25}$$

where $a_j (j = 0, 1, 2, 3, \dots, P)$. The homogeneous balancing technique can be used to obtain the value of P by maintaining the balance between the derivative term and the highest order nonlinear term in equation (3.24). Consequently $\frac{d^w u}{d\xi^w}$, maximum degree is categorized as follows:

$$F(\frac{d^w M}{d\xi^w}) = n + w.$$
$$F(N^f \frac{d^w M}{d\xi^w})^s = fn + s(n + w).$$

The Equation (3.25) considers the $\phi(\xi)$ to be the solution to the following equation:

$$(\phi')^2(\xi) = d_2\phi^4(\xi) + d_1\phi^2(\xi) + d_0, \tag{3.26}$$

where the constants $d_n, n = 0, 1, 2$ must be computed; further details on equation (3.26) are available in[29]. This set of solutions satisfied equation (3.26) using F as the integration constant:

Case 1:

Rational solutions for $d_0 = d_1 = 0$ and $d_2 > 0$.

$$\phi_1(\xi) = \pm \frac{1}{\sqrt{d_2}(\xi + F)}. \tag{3.27}$$

Case 2:

Exponential solutions for $d_0 = 0$ and $d_1 > 0$.

$$\phi_2(\xi) = \frac{4d_1 e^{\pm\sqrt{d_1}(\xi+F)}}{e^{\pm 2\sqrt{d_1}(\xi+F)} - 4d_1 d_2}, \tag{3.28}$$

$$\phi_3(\xi) = \frac{4d_1 e^{\pm\sqrt{d_1}(\xi+F)}}{1 - 4d_1 d_2 e^{\pm 2\sqrt{d_1}(\xi+F)}}. \tag{3.29}$$

Case 3:

Trigonometric hyperbolic solutions:

(i) For $d_0 = 0, d_1 > 0$ and $d_2 \neq 0$,

$$\phi_4(\xi) = \pm\sqrt{-\frac{d_1}{d_2}}\,\mathrm{sech}(d_1(\xi + F)), \tag{3.30}$$

$$\phi_5(\xi) = \pm\sqrt{\frac{d_1}{d_2}}\,\mathrm{csch}(d_1(\xi + F)). \tag{3.31}$$

(ii) For $d_0 = \frac{b_1^2}{4d_2}, d_1 < 0$ and $b_2 > 0$,

$$\phi_6(\xi) = \pm\sqrt{-\frac{d_1}{2d_2}}\tanh(\sqrt{-\frac{d_1}{2}}(\xi + F)), \tag{3.32}$$

$$\phi_7(\xi) = \pm\sqrt{-\frac{d_1}{2d_2}}\coth(\sqrt{-\frac{d_1}{2}}(\xi + F)), \tag{3.33}$$

$$\phi_8(\xi) = \pm\sqrt{-\frac{d_1}{2d_2}}(\tanh(\sqrt{-2d_1}(\xi + F)) \pm i\,\mathrm{sech}(\sqrt{-2d_1}(\xi + F)), \tag{3.34}$$

$$\phi_9(\xi) = \pm\sqrt{-\frac{d_1}{2d_2}}(\coth(\sqrt{-2d_1}(\xi + F)) \pm \mathrm{csch}(\sqrt{-2d_1}(\xi + F)), \tag{3.35}$$

$$\phi_{10}(\xi) = \pm\sqrt{-\frac{d_1}{8d_2}}(\tanh(\sqrt{-\frac{d_1}{8}}(\xi+F)+\coth(\sqrt{-\frac{d_1}{8}}(\xi+F)). \tag{3.36}$$

Case 4:
Trigonometric functions.

(i) For $d_0 = 0, d_1 < 0$ and $d_2 \neq 0$,

$$\phi_{11}(\xi) = \pm\sqrt{-\frac{d_1}{d_2}}\sec(\sqrt{-d_1}(\xi+F)), \tag{3.37}$$

$$\phi_{12}(\xi) = \pm\sqrt{-\frac{d_1}{d_2}}\csc(\sqrt{-d_1}(\xi+F)). \tag{3.38}$$

(ii) For $d_0 = \frac{b_1^2}{4d_2}, d_1 > 0$ and $d_2 > 0$,

$$\phi_{13}(\xi) = \pm\sqrt{\frac{d_1}{2d_2}}\tan(b\frac{d_1}{2}(\xi+F)), \tag{3.39}$$

$$\phi_{14}(\xi) = \pm\sqrt{\frac{d_1}{2d_2}}\cot(\sqrt{\frac{d_1}{2}}(\xi+F)), \tag{3.40}$$

$$\phi_{15}(\xi) = \pm\sqrt{\frac{d_1}{2d_2}}(\tan(\sqrt{2d_1}(\xi+F))\pm\sec(\sqrt{2d_1}(\xi+F)), \tag{3.41}$$

$$\phi_{16}(\xi) = \pm\sqrt{\frac{d_1}{2d_2}}(\cot(\sqrt{2d_1}(\xi+F))\pm\csc(\sqrt{2d_1}(\xi+F)), \tag{3.42}$$

$$\phi_{17}(\xi) = \pm\sqrt{\frac{d_1}{8d_2}}(\tan(\sqrt{\frac{d_1}{8}}(\xi+F))-\cot(\sqrt{\frac{d_1}{8}}(\xi+F)). \tag{3.43}$$

By putting equations (3.23) and equation (3.24) into equation (3.22) and after setting all of the coefficients for each power of $\phi(\xi)$ to zero, Computational software Mathematica 13.2 was used to solve the resulting system of algebraic equations. Ultimately, added these constants to equation (3.23) and derived distinct solutions as indicated in equations (3.27)-(3.43). Consequently, various exact solutions for NLPDEs were obtained.

Comparative study of IMSSEM and GAEM

The generalized auxiliary equation method provides a simple and efficient method of designing exact analytical solutions to nonlinear evolution equations. The key advantage of generalized auxiliary equation method is its simplicity and reduced computational requirement. With the introduction of an auxiliary differential equation whose general solutions are known, GAEM has the ability to readily deliver closed-form solutions of solitons as well as periodic wave patterns. The technique is subject to very little symbolic manipulation, so it can be used effectively for quick analytical exploration or preliminary testing of nonlinear models. Yet its greatest limitation is that it won't always accurately model complex or high-order interactions and becomes unwieldy with large numbers of parameters.

Contrary to these, the IMSSEM increases the flexibility and range of the traditional analytical methods by using adjustable parameters and enhanced balancing conditions. This makes it possible for IMSSEM to obtain a more diverse class of nonlinear wave solutions such as bright, dark, kink, anti-kink, periodic, M-type, and W-type solitons. The technique can deal well with higher-order and mixed nonlinearities, which are typically found in complicated physical systems like plasma waves and optical fibers. However, IMSSEM is more algebraically and computationally intensive and needs symbolic software for dealing with long expressions and parameter tuning. Even with its more substantial computational burden, IMSSEM offers greater accuracy and flexibility and is especially important for studying intricate soliton forms, stability dynamics, and parameter sensitivity in nonlinear dynamical systems. Its limitation is algebraic complexity–derivations can be excessively long, and the procedure may need symbolic computation methods for tractability.

Applications of methods

Applications of generalized auxiliary equation method

Assume that the solutions to equation (1.1) in the traveling wave form are

$$\begin{aligned} w(x,t) =&\phi(\xi)e^{iQ(x,t)}, \\ \phi(\xi) =&a_0 + \sum_{i=1}^{J} a_1 \varpi^i(\xi) \\ ,\xi =&sx + pt, \\ Q(x,t) =&\alpha x + \gamma t + \theta, \end{aligned} \tag{4.1}$$

$$\varpi'(\xi) = \sqrt{q_1\varpi(\xi)^2 + q_2\varpi(\xi)^3 + q_3\varpi(\xi)^4}. \tag{4.2}$$

Apply the homogeneous balancing principle in equation (2.2) and assume the solution of equation(2.2) as

$$\phi(\xi) = a_0 + a_1\varpi(\xi) \tag{4.3}$$

By inserting equation (4.3) into equation (2.2), the system of equations is produced. The following sets of solutions are found by solving the system of equations.

Set-1

$$a_0 = 0, a_1 = \frac{k\sqrt{6}\sqrt{\delta}\sqrt{q_3}}{\sqrt{\beta_1 - \delta\beta_2}}, \gamma = \alpha^3 - 3s^2\alpha q_1 + 3a_0^2\beta_1 - 3\alpha a_0^2\beta_2. \tag{4.4}$$

The following solutions are obtained by combining equation (4.4) with equations ((3.6)–(3.21) and (4.3).

Trigonometric hyperbolic solutions

$$w_1(\xi) = \left(\frac{k\sqrt{6}\sqrt{\delta}\sqrt{q_3}}{\sqrt{\beta_1 - \delta\beta_2}}\right)\left(\frac{-q_1q_2\text{sech}^2(\frac{\sqrt{q_1}}{2}\xi)}{q_2^2 - q_1q_3(1 \pm \tanh(\frac{\sqrt{q_1}}{2}\xi))}\right)e^{iQ(x,t)}, b_1 > 0. \tag{4.5}$$

$$w_2(\xi) = \left(\frac{k\sqrt{6}\sqrt{\delta}\sqrt{q_3}}{\sqrt{\beta_1 - \delta\beta_2}}\right)\left(\frac{q_1q_2\text{csch}^2(\frac{\sqrt{q_1}}{2}\xi)}{q_2^2 - q_1q_3(1 \pm \coth(\frac{\sqrt{q_1}}{2}\xi))}\right)e^{iQ(x,t)}, b_1 > 0. \tag{4.6}$$

$$\begin{aligned} w_3(\xi) =&\left(\frac{k\sqrt{6}\sqrt{\delta}\sqrt{q_3}}{\sqrt{\beta_1 - \delta\beta_2}}\right)\left(\frac{2q_1\text{sech}^2(\sqrt{q_1}\xi)}{\pm\sqrt{\zeta} - q_2\text{sech}(\sqrt{q_1}\xi)}\right)e^{iQ(x,t)}, q_1 > 0, \zeta > 0. \\ w_4(\xi) =&\left(\frac{k\sqrt{6}\sqrt{\delta}\sqrt{q_3}}{\sqrt{\beta_1 - \delta\beta_2}}\right)\left(\frac{2q_1\text{sech}^2(\sqrt{q_1}\xi)}{\pm\sqrt{-\zeta} - q_2\text{sech}(\sqrt{q_1}\xi)}\right)e^{iQ(x,t)}, q_1 > 0, \zeta > 0. \\ w_5(\xi) =&\left(\frac{k\sqrt{6}\sqrt{\delta}\sqrt{q_3}}{\sqrt{\beta_1 - \delta\beta_2}}\right)\left(\frac{-q_1\text{sech}^2(\frac{\sqrt{q_1}}{2}\xi)}{q_2 \pm 2\sqrt{q_1q_3}\tanh(\frac{\sqrt{q_1}}{2}\xi)}\right)e^{iQ(x,t)}, q_1 > 0, q_3 > 0. \\ w_6(\xi) =&\left(\frac{k\sqrt{6}\sqrt{\delta}\sqrt{q_3}}{\sqrt{\beta_1 - \delta\beta_2}}\right)\left(\frac{q_1\text{csch}^2(\frac{\sqrt{q_1}}{2}\xi)}{q_2 \pm 2\sqrt{q_1q_3}\coth(\frac{\sqrt{q_1}}{2}\xi)}\right)e^{iQ(x,t)}, q_1 > 0, q_3 > 0. \end{aligned} \tag{4.7}$$

$$\begin{aligned} w_7(\xi) =&\left(\frac{k\sqrt{6}\sqrt{\delta}\sqrt{q_3}}{\sqrt{\beta_1 - \delta\beta_2}}\right)\left(-\frac{q_1}{q_2}(1 \pm \tanh(\frac{\sqrt{q_1}}{2}\xi))\right)e^{iQ(x,t)}, q_1 > 0, \zeta = 0. \\ w_8(\xi) =&\left(\frac{k\sqrt{6}\sqrt{\delta}\sqrt{q_3}}{\sqrt{\beta_1 - \delta\beta_2}}\right)\left(-\frac{q_1}{q_2}(1 \pm \coth(\frac{\sqrt{q_1}}{2}\xi))\right)e^{iQ(x,t)}, q_1 > 0, \zeta = 0. \end{aligned} \tag{4.8}$$

Trigonometric solutions

$$\begin{aligned} w_9(\xi) =&\left(\frac{k\sqrt{6}\sqrt{\delta}\sqrt{q_3}}{\sqrt{\beta_1 - \delta\beta_2}}\right)\left(\frac{-q_1\sec^2(\frac{\sqrt{-q_1}}{2}\xi)}{q_2 \pm 2\sqrt{-q_1q_3}(\tan(\frac{\sqrt{-q_1}}{2}\xi)}\right)e^{iQ(x,t)}, q_1 > 0, q_3 > 0. \\ w_{10}(\xi) =&\left(\frac{k\sqrt{6}\sqrt{\delta}\sqrt{q_3}}{\sqrt{\beta_1 - \delta\beta_2}}\right)\left(\frac{-q_1\csc^2(\frac{\sqrt{-q_1}}{2}\xi)}{q_2 \pm 2\sqrt{-q_1q_3}(\cot(\frac{\sqrt{-q_1}}{2}\xi)}\right)e^{iQ(x,t)}, q_1 > 0, q_3 > 0. \\ w_{11}(\xi) =&\left(\frac{k\sqrt{6}\sqrt{\delta}\sqrt{q_3}}{\sqrt{\beta_1 - \delta\beta_2}}\right)\left(\frac{2q_1\sec^2(\sqrt{-q_1}\xi)}{\pm\zeta - b_2\sec(\sqrt{-q_1}\xi)}\right)e^{iQ(x,t)}, q_1 > 0, \zeta > 0. \\ w_{12}(\xi) =&\left(\frac{k\sqrt{6}\sqrt{\delta}\sqrt{q_3}}{\sqrt{\beta_1 - \delta\beta_2}}\right)\left(\frac{2q_1\csc^2(\sqrt{-q_1}\xi)}{\pm\zeta - b_2\sec(\sqrt{-q_1}\xi)}\right)e^{iQ(x,t)}, q_1 > 0, \zeta > 0. \end{aligned}$$

Exponential solutions

$$w_{13}(\xi) = \left(\frac{k\sqrt{6}\sqrt{\delta}\sqrt{q_3}}{\sqrt{\beta_1 - \delta\beta_2}}\right)\left(\frac{4q_1 e^{\pm\sqrt{q_1}\xi}}{(e^{\pm\sqrt{q_1}\xi} - q_2)^2 - 4q_1 q_3}\right)e^{iQ(x,t)}, q_1 > 0.$$
$$w_{14}(\xi) = \left(\frac{k\sqrt{6}\sqrt{\delta}\sqrt{q_3}}{\sqrt{\beta_1 - \delta\beta_2}}\right)\left(\frac{\pm 4q_1 e^{\pm\sqrt{q_1}\xi}}{1 - 4q_1 q_3 e^{\pm 2\sqrt{q_1}\xi}}\right)e^{iQ(x,t)}, q_1 > 0, q_2 = 0. \tag{4.9}$$

Rational solutions

$$w_{15}(\xi) = \left(\frac{k\sqrt{6}\sqrt{\delta}\sqrt{q_3}}{\sqrt{\beta_1 - \delta\beta_2}}\right)\left(\frac{\pm q_1 q_2}{q_2^2\varkappa^2 - q_1 q_3}\right)e^{iQ(x,t)}, q_1 > 0.$$
$$w_{16}(\xi) = \left(\frac{k\sqrt{6}\sqrt{\delta}\sqrt{q_3}}{\sqrt{\beta_1 - \delta\beta_2}}\right)\left(\pm\frac{1}{\sqrt{q_3}\xi}\right)e^{iQ(x,t)}, q_1 = 0, q_2 = 0. \tag{4.10}$$

Applications of IMSSEM

Assume that the solutions to equation (1.1) in the traveling wave form are

$$u(x,t) = \phi(\xi)e^{iQ(x,t)}, \phi(\xi) = a_0 + \sum_{i=1}^{J} a_1\phi^i(\xi)$$
$$, \xi = sx + pt, Q(x,t) = \alpha x + \gamma t + \theta,$$

Apply the homogeneous balancing principle in equation (2.2) and take the answer to equation (2.2) as

$$\phi(\xi) = a_0 + a_1\varpi(\xi) \tag{4.11}$$

The system of equations is obtained by putting equation (4.12) into equation (2.2). Solving the system of equations, then the following set of solutions are obtained.

Set-1

$$a_0 = 0, a_1 = \frac{k\sqrt{6}\sqrt{\delta}\sqrt{d_2}}{\sqrt{\beta_1 - \delta\beta_2}}, \gamma = \alpha^3 - 3s^2\alpha d_1 + 3a_0^2\beta_1 - 3\alpha a_0^2\beta_2. \tag{4.12}$$

The following solutions are obtained by combining equation (4.12) with equations ((3.27)–(3.43).

Case 1:

For $d_0 = d_1 = 0$ and $d_2 > 0$. The rational solutions will have the following structure:

$$u_1(\xi) = \left(\frac{k\sqrt{6}\sqrt{\delta}\sqrt{d_2}}{\sqrt{\beta_1 - \delta\beta_2}}\right)\left(\pm\frac{1}{\sqrt{d_2}(\xi + F)}\right)e^{iQ(x,t)}.$$

Case 2:

For $d_0 = 0$ and $d_1 > 0$.The exponential solutions will have the following form:

$$u_2(\xi) = \left(\frac{k\sqrt{6}\sqrt{\delta}\sqrt{d_2}}{\sqrt{\beta_1 - \delta\beta_2}}\right)\left(\frac{4d_1 e^{\pm\sqrt{d_1}(\xi+F)}}{e^{\pm 2\sqrt{d_1}(\xi+F)} - 4d_1 d_2}\right)e^{iQ(x,t)},$$
$$u_3(\xi) = \left(\frac{k\sqrt{6}\sqrt{\delta}\sqrt{d_2}}{\sqrt{\beta_1 - \delta\beta_2}}\right)\left(\frac{4d_1 e^{\pm\sqrt{d_1}(\xi+F)}}{1 - 4d_1 d_2 e^{\pm 2\sqrt{d_1}(\xi+F)}}\right)e^{iQ(x,t)}.$$

Case 3:

The following are the trigonometric hyperbolic solutions:

(i) For $d_0 = 0, d_1 > 0$ and $d_2 \neq 0$,

$$u_4(\xi) = \left(\frac{k\sqrt{6}\sqrt{\delta}\sqrt{d_2}}{\sqrt{\beta_1 - \delta\beta_2}}\right)\left(\pm\sqrt{-\frac{d_1}{d_2}}\operatorname{sech}(d_1(\xi + F))\right)e^{iQ(x,t)},$$
$$u_5(\xi) = \left(\frac{k\sqrt{6}\sqrt{\delta}\sqrt{d_2}}{\sqrt{\beta_1 - \delta\beta_2}}\right)\left(\pm\sqrt{\frac{d_1}{d_2}}\operatorname{csch}(d_1(\xi + F))\right)e^{iQ(x,t)}. \tag{4.13}$$

(ii) For $d_0 = \frac{b_1^2}{4d_2}, d_1 < 0$ and $b_2 > 0$,

$$u_6(\xi) = \left(\frac{k\sqrt{6}\sqrt{\delta}\sqrt{d_2}}{\sqrt{\beta_1 - \delta\beta_2}}\right)\left(\pm\sqrt{-\frac{d_1}{2d_2}}\tanh\left(\sqrt{-\frac{d_1}{2}}(\xi + F)\right)\right)e^{iQ(x,t)}, \tag{4.14}$$

$$
\begin{aligned}
u_7(\xi) =& \left(\frac{k\sqrt{6}\sqrt{\delta}\sqrt{d_2}}{\sqrt{\beta_1-\delta\beta_2}}\right)\left(\pm\sqrt{-\frac{d_1}{2d_2}}\coth(\sqrt{-\frac{d_1}{2}}(\xi+F))\right)e^{iQ(x,t)},\\
u_8(\xi) =& \left(\frac{k\sqrt{6}\sqrt{\delta}\sqrt{d_2}}{\sqrt{\beta_1-\delta\beta_2}}\right)\left(\pm\sqrt{-\frac{d_1}{2d_2}}(\tanh(\sqrt{-2d_1}(\xi+F))\pm i\,\mathrm{sech}(\sqrt{-2d_1}(\xi+F))\right)e^{iQ(x,t)},\\
u_9(\xi) =& \left(\frac{k\sqrt{6}\sqrt{\delta}\sqrt{d_2}}{\sqrt{\beta_1-\delta\beta_2}}\right)\left(\pm\sqrt{-\frac{d_1}{2d_2}}(\coth(\sqrt{-2d_1}(\xi+F))\pm \mathrm{csch}(\sqrt{-2d_1}(\xi+F))\right)e^{iQ(x,t)},
\end{aligned}
\tag{4.15}
$$

$$
u_{10}(\xi) = \left(\frac{k\sqrt{6}\sqrt{\delta}\sqrt{d_2}}{\sqrt{\beta_1-\delta\beta_2}}\right)\left(\pm\sqrt{-\frac{d_1}{8d_2}}(\tanh(\sqrt{-\frac{d_1}{8}}(\xi+F)+\coth(\sqrt{-\frac{d_1}{8}}(\xi+F))\right)e^{iQ(x,t)}.
\tag{4.16}
$$

Case 4:

Below are the solutions that have the shape of trigonometric functions:

(i) For $d_0 = 0, d_1 < 0$ and $d_2 \neq 0$,

$$
\begin{aligned}
u_{11}(\xi) =& \left(\frac{k\sqrt{6}\sqrt{\delta}\sqrt{d_2}}{\sqrt{\beta_1-\delta\beta_2}}\right)\left(\pm\sqrt{-\frac{d_1}{d_2}}\sec(\sqrt{-d_1}(\xi+F))\right)e^{iQ(x,t)},\\
u_{12}(\xi) =& \left(\frac{k\sqrt{6}\sqrt{\delta}\sqrt{d_2}}{\sqrt{\beta_1-\delta\beta_2}}\right)\left(\pm\sqrt{-\frac{d_1}{d_2}}\csc(\sqrt{-d_1}(\xi+F))\right)e^{iQ(x,t)}.
\end{aligned}
$$

(ii) For $d_0 = \frac{b_1^2}{4d_2}, d_1 > 0$ and $d_2 > 0$,

$$
\begin{aligned}
u_{13}(\xi) =& \left(\frac{k\sqrt{6}\sqrt{\delta}\sqrt{d_2}}{\sqrt{\beta_1-\delta\beta_2}}\right)\left(\pm\sqrt{\frac{d_1}{2d_2}}\tan(b\frac{d_1}{2}(\xi+F))\right)e^{iQ(x,t)},\\
u_{14}(\xi) =& \left(\frac{k\sqrt{6}\sqrt{\delta}\sqrt{d_2}}{\sqrt{\beta_1-\delta\beta_2}}\right)\left(\pm\sqrt{\frac{d_1}{2d_2}}\cot(\sqrt{\frac{d_1}{2}}(\xi+F))\right)e^{iQ(x,t)},\\
u_{15}(\xi) =& \left(\frac{k\sqrt{6}\sqrt{\delta}\sqrt{d_2}}{\sqrt{\beta_1-\delta\beta_2}}\right)\left(\pm\sqrt{\frac{d_1}{2d_2}}(\tan(\sqrt{2d_1}(\xi+F))\pm\sec(\sqrt{2d_1}(\xi+F))\right)e^{iQ(x,t)},\\
u_{16}(\xi) =& \left(\frac{k\sqrt{6}\sqrt{\delta}\sqrt{d_2}}{\sqrt{\beta_1-\delta\beta_2}}\right)\left(\pm\sqrt{\frac{d_1}{2d_2}}(\cot(\sqrt{2d_1}(\xi+F))\pm\csc(\sqrt{2d_1}(\xi+F))\right)e^{iQ(x,t)},\\
u_{17}(\xi) =& \left(\frac{k\sqrt{6}\sqrt{\delta}\sqrt{d_2}}{\sqrt{\beta_1-\delta\beta_2}}\right)\left(\pm\sqrt{\frac{d_1}{8d_2}}(\tan(\sqrt{\frac{d_1}{8}}(\xi+F))-\cot(\sqrt{\frac{d_1}{8}}(\xi+F))\right)e^{iQ(x,t)}.
\end{aligned}
$$

Visual evaluations and discussion

In this study, the generalized third-order NLSE was solved using the generalized auxiliary equation method and IMSSEM. A variety of solitary waves, including periodic, dark soliton, bright soliton, kink soliton, anti-kink soliton, bell and anti-bell solitons, can be produced using the aforementioned procedures. Graphical plots of some results have been employed here to emphasize their dynamic nature with parameters appropriately chosen.

In Fig. 1, the anti-kink soliton solution is displayed when $s = 1, p = 1, \alpha = -3, q_1 = 2, q_2 = 2, q_3 = 1, \beta_1 = 2, \beta_2 = 3$, and $\theta = 1$. Anti-kink soliton solutions are waves that go from a nonzero value to zero, contrary to kink solitons.

In Fig. 2, the singular soliton solution is displayed when $s = 1, p = 1, \alpha = 2, q_1 = 2, q_2 = 1, q_3 = 1, \beta_1 = 1, \beta_2 = 3$, and $\theta = 2$. Singular solitons lead to solutions with a singularity in their shape, like a discontinuity or an infinite peak.

In Fig. 3, the bell type soliton solution is displayed when $s = -1, p = -1, \alpha = -2, q_1 = 2, q_2 = 1, q_3 = -1, \beta_1 = 1, \beta_2 = 4$, and $\theta = 2$. Waves with a peak localized in the nonlinear medium which moves called bell type solitons.

In Fig. 4, the kink soliton solution is displayed when $s = -1, p = -1, \alpha = 4, q_1 = 1, q_2 = 3, q_3 = 2, \beta_1 = 1, \beta_2 = 3$, and $\theta = 1$. A wave which smoothly and smoothly passes from one such state to another without oscillation. known as a kink-type soliton.

In Fig. 5, the periodic soliton solution is displayed when $s = 1, p = 1, \alpha = 2.5, q_1 = 2, q_2 = 0, q_3 = -9, \beta_1 = 1, \beta_2 = 6$, and $\theta = 1$. They are also solutions designated as cnoidal waves, i.e., periodic solitons. pattern in either space or time. Periodic solitons expand while bright solitons are spatially localized.

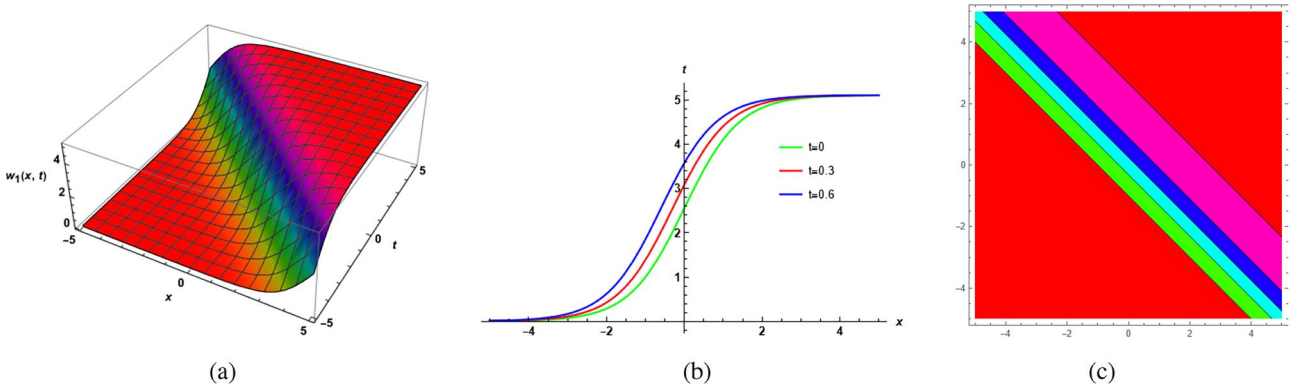

(a) (b) (c)

Fig. 1. Equation (4.5) yields a solution for $w_1(x,t)$, which is an anti-kink soliton solution.

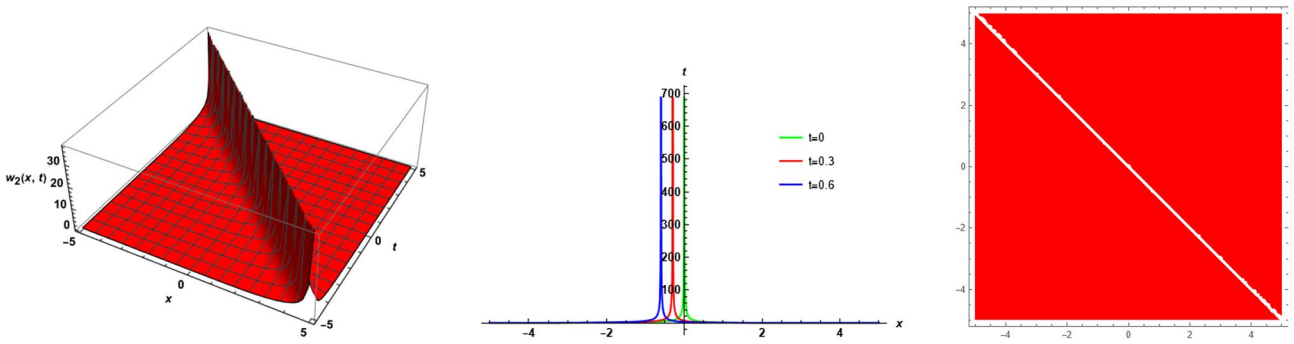

(a) (b) (c)

Fig. 2. Equation (4.6) yields a solution for $w_2(x,t)$, which is a singular type soliton solution.

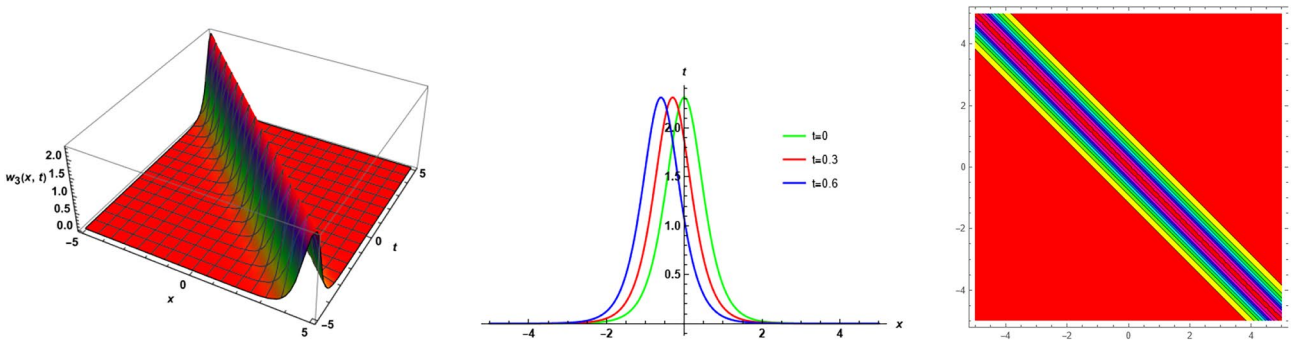

(a) (b) (c)

Fig. 3. Equation (4.7) provides a solution for $w_3(x,t)$, which is a bell type soliton solution.

In Fig. 6, the singular soliton solution is displayed when $s=1, p=1, \alpha=1, q_1=0, q_2=0, q_3=1, \beta_1=1, \beta_2=3$, and $\theta=1$. Solutions with a singularity in their shape, i.e. a discontinuity or an infinite peak.

In Fig. 7, the bell type soliton solution is displayed when $s=1, p=-1, \alpha=-0.3, d_1=5, d_2=-2, \beta_1=-2, \beta_2=0.3, F=0.2$ and $\theta=1$.

In Fig. 8, a dark soliton solution is displayed when $s=1, p=1, \alpha=0.3, d_1=-1, d_2=2, \beta_1=2, \beta_2=0.3, F=1$ and $\theta=1$ and $\theta=1$.

In Fig. 9, the M-type soliton solution is displayed when $s=1, p=1, \alpha=1, d_1=-1, d_2=8, \beta_1=0.2, \beta_2=0.1$, F=0.01 and $\theta=1$.

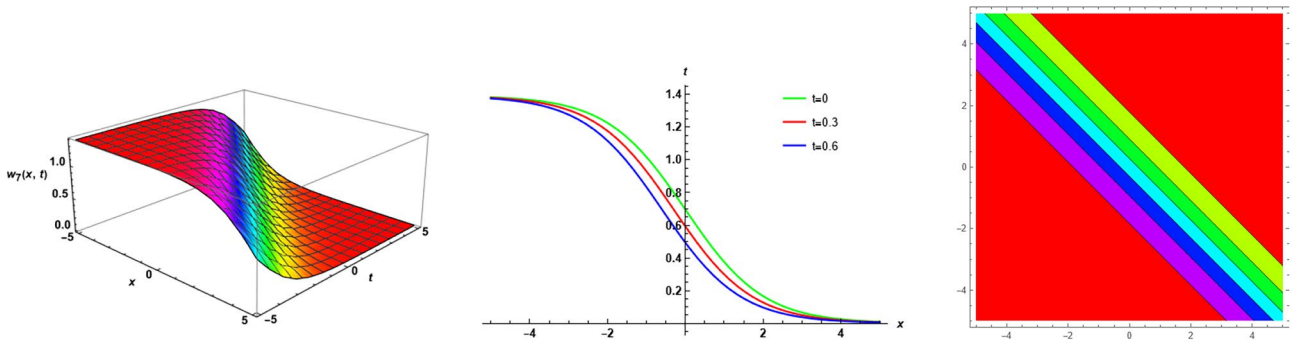

(a) (b) (c)

Fig. 4. Equation (4.8) gives a solution for $w_7(x,t)$, which is a kink soliton solution.

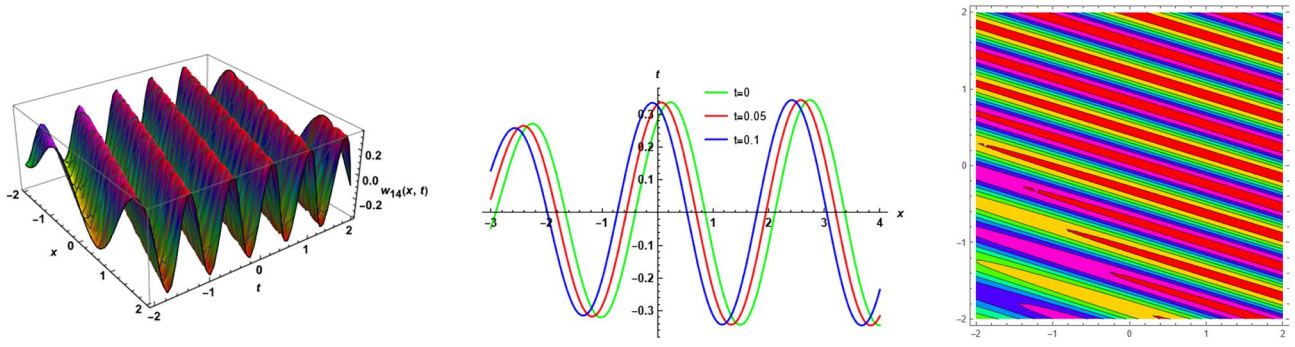

(a) (b) (c)

Fig. 5. Equation (4.9) yields a solution for $w_{14}(x,t)$, which is a periodic soliton solution.

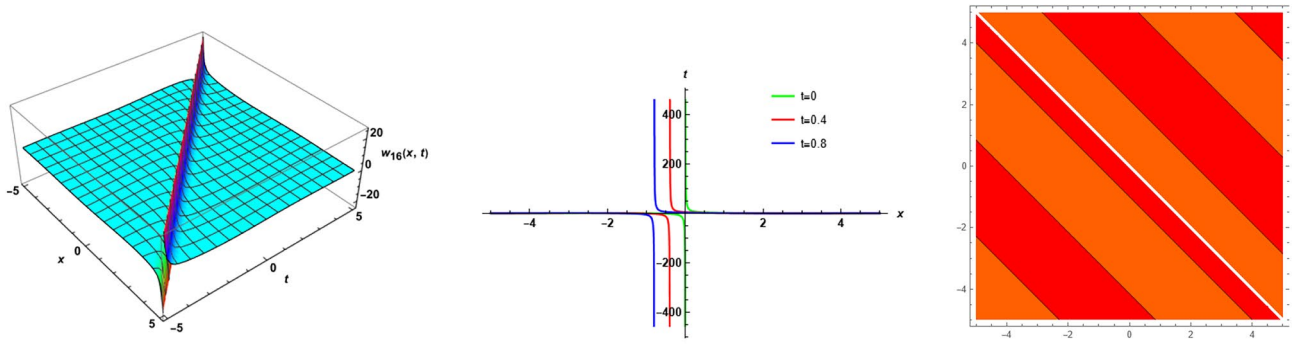

(a) (b) (c)

Fig. 6. Equation (4.10) yields a solution for $w_{16}(x,t)$, which is a singular soliton solution.

In Fig. 10, the W-type soliton solution is displayed $s=1, p=1, \alpha=0.3, d_1=-1, d_2=0.2, F=0.1, \beta_1=2, \beta_2=-1$ and $\theta=1$.

Physical interpretation

Many branches of science rely on the nonlinear Schrödinger equations, which a class of nonlinear evolution equations. There are many intricate changes in nature that this equation can effectively depict.

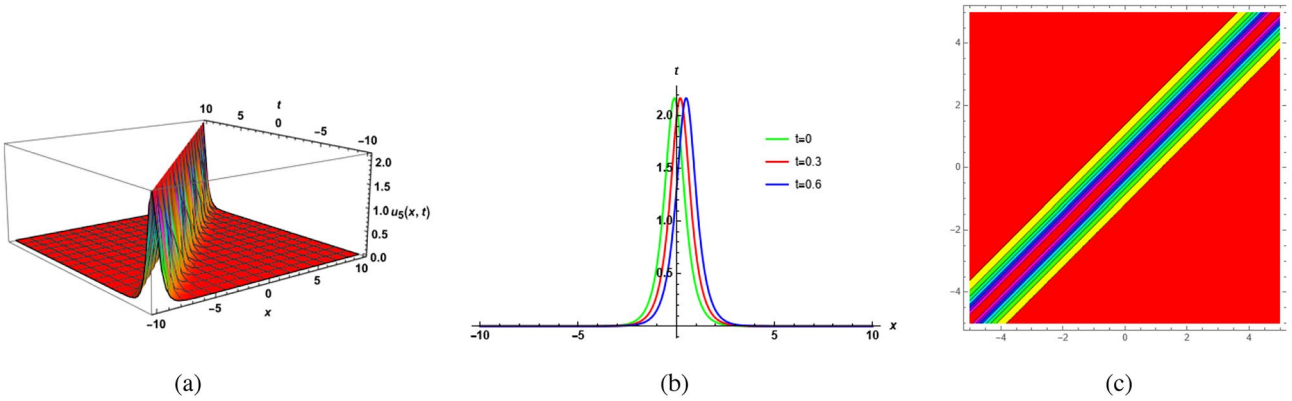

Fig. 7. Equation (4.13) yields a solution for $u_5(x, t)$, which is a bright or bell soliton solution.

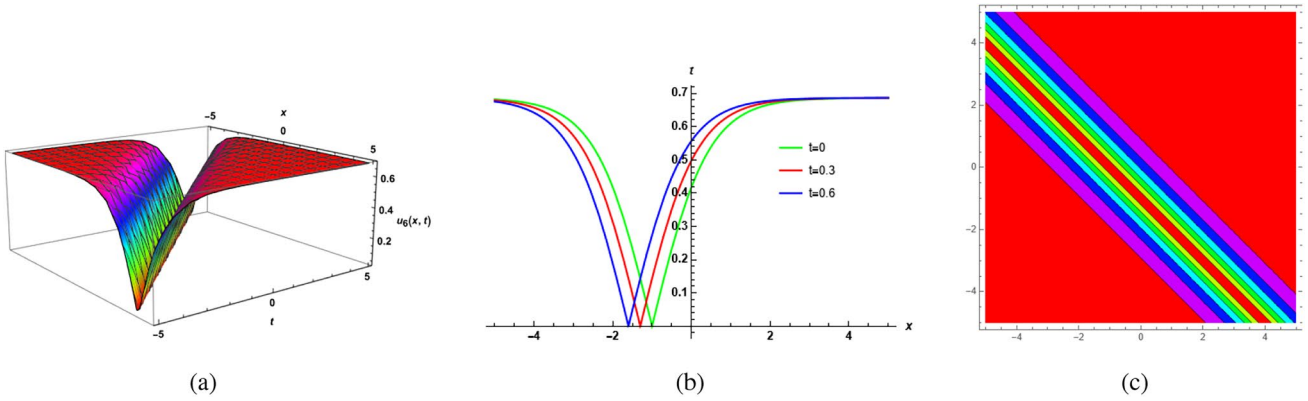

Fig. 8. Equation (4.14) yields a 3*D* animation of $u_6(x, t)$, which is a dark soliton solution.

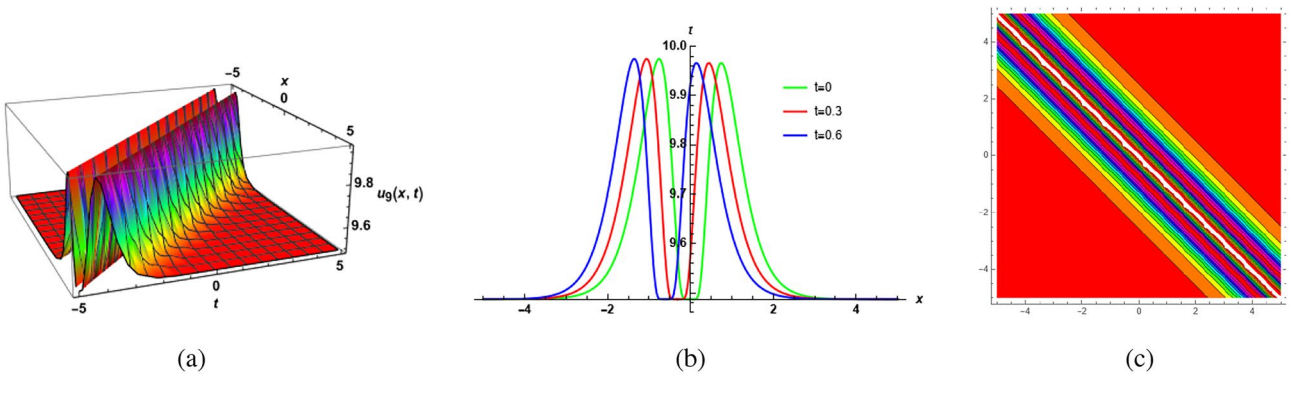

Fig. 9. Equation (4.15) yields a 3*D* animation of $u_9(x, t)$, which is a M-type soliton solution.

Kink Soliton

An anti-kink, which is merely a phase shift in the direction of a kink, is shown in Fig. 1. More precisely, an anti-kink moves from a higher value to a lower value, whereas a kink moves from a lower value to a higher value. Kinks and anti-kinks both cause localized disturbances and their energy densities are significantly different from those of the surrounding environment. In a nonlinear system, the anti-kink is a localized structure that functions in the opposite manner from the kink, just like its counterpart. The dynamics of the system may be impacted by this energy density differential because anti-kinks are a system reversal or phase shift. These localized patterns are responsible for the complex behaviors observed in a variety of physical environments and are crucial in capturing the nonlinear coupling and energy flow in such systems. In plasma physics, kink solitons are used to explain shock-like or transition fronts that result from energy transfer processes. Their stability and resistance

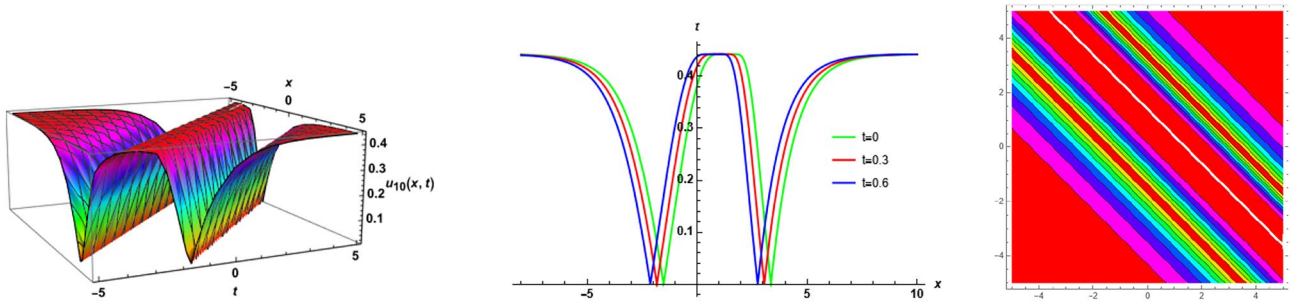

Fig. 10. Equation (4.16) gives a solution for $u_{10}(x, t)$, which is a W-shape soliton solution.

to perturbations make them of utility in modeling information transmission and energy transport in dispersive and nonlinear media.

Singular Soliton

In Figs. 2 and 6, Singular soliton solutions are a specific kind of soliton solution to nonlinear partial differential equations that feature singularities, meaning that they have extreme behavior (such infinite gradients or discontinuities) or points where the solution is indeterminate. Singularities can entail phenomena like blowup, where some properties (such amplitude) increase without bounds within a finite time and the solution collapses, even though normal solitons are stable, localized waves that maintain their shape over time.

Bell-shaped Soliton

Since the bell-shaped solitons in Fig. 3 have few stable wave patterns, they are widely used in many scientific domains. These solitary wave transmissions, known as solitons, can move across long distances without changing their shape. Bell-shaped solitons possess a localized peak in the amplitude of the wave, which is an intensity or energy concentration at a single point. As seen in Fig. 4, a kink soliton represents a localized, stable transition between two different states of a system and provides a solution to certain nonlinear field equations. In fields like condensed matter physics, field theory, and nonlinear dynamics, these solutions are very significant.

Periodic Soliton

Figure 5 depicts periodic solitons, a kind of wave pattern that recurs repeatedly in space and time. Due to the nonlinear nature of the system, the waves maintain their shape and coherence over long distances. They model shallow water waves, coastal regions and tsunamis using fluid dynamics. In the area of nonlinear optics, they describe the constant streams of light in lasers and optical fibers.

Bright Soliton

Figure 7 depicts a bell or bright soliton, A bright soliton, or a bell soliton due to its bell-shaped profile, is a soliton solution that commonly occurs in nonlinear wave equations. Bright solitons possess a localized peak in the amplitude of the wave, which is an intensity or energy concentration at a single point. Contrary to dark solitons, which are shown by holes or troughs in the wave profile, bright solitons are positive perturbations, where the intensity of the wave is highest at the center and drops outward in a smooth fashion.

Dark Soliton

A dark soliton, as shown in Figure 8, is a confined perturbation in a wave medium that maintains a continuous phase structure while having a small amplitude at its center. Wave propagation in specific nonlinear media is described by these solitons, which are solutions to NLPDEs, such as the NLSE.

M-type Soliton

Figure 9 depicts an M-type soliton, has a wave profile shaped like the letter M usually consisting of two peaks with a dip in between. M-shape solitons are more complex than normal solitons, which are single-peaked and maintain their shape as they move, with an intermediate dip between two separate maxima. This shape is an indication of energy splitting inside the pulse, with the result being the presence of two intensity peaks. In optical communications, M-type solitons are crucial for the understanding of pulse shaping, two-channel transmission, and nonlinear cross-coupling effects. In plasma physics, M-type solitons signify the nonlinear coupling of different wave modes, which explains wave propagation of multi-structure and energy sharing effects.

W-type Soliton

Frequent W-shaped soliton patterns occur in both the spatial and temporal domains as shown in Fig. 10. A distinctively shaped W- soliton is characterized by two symmetrical valleys flanking a central spike. A discreet, nonlinear wave that's dependent on only a specific area. These solitons enable the representation of rapid and precise data transfers over long distances. For challenges encountered in optical fiber systems, such solitons are highly practical. They may vary between static and oscillatory behaviors, with a waveform similar to that of a rogue

wave yet more deterministic and reliable. These solutions explain periodic energy localization and are capable of simulating modulation instability or repeated pulse creation in nonlinear media. In optical fiber, W-type solitons can be applied to the investigation of pulse compression and stability in high-dispersion regimes, and in plasma physics, they map to nonlinear oscillations representing energy confinement and periodic wave modulation. The values of parameters β_1, β_2, and β_3 third-order dispersion, self-steepening, and nonlinear dispersion were set in physically realistic ranges so that the system would be stable and be able to capture important dynamics of the generalized third-order NLSE. Sensitivity analysis reveals that β_1 primarily produces phase shifts, β_1 produces pulse asymmetry, and β_1 generates multi-hump and oscillatory solitons. Simultaneous increases in β_2 and β_3 induce bifurcations and potential instabilities, demonstrating how higher-order effects control soliton behavior.

Dynamical analysis

This section investigates the system's dynamic complexity through bifurcation analysis, chaotic dynamics and sensitivity analysis. Bifurcation analysis is applied to locate the parameter values responsible for significant changes in system behavior.

Bifurcation analysis

A graphic representation of the bifurcation and phase diagrams of the planar dynamical system is presented in this section. This approach of dynamical systems can be used to qualitatively assess nonlinear partial differential models. The orbits of the system can take the form of simple closed curves, points, or other isomorphic structures. Given a Hamiltonian function and the assumption that $\frac{d\phi}{d\xi} = P$, in its planar dynamic version can be expressed as follows:

$$\frac{d\phi}{d\xi} = P, \frac{dP}{d\xi} = l_1\phi + l_2\phi^3. \tag{7.1}$$

$$H(\phi, P) = \frac{P^2}{2} - l_1\frac{\phi^2}{2} - l_2\frac{\phi^4}{4} = g, \tag{7.2}$$

whereas $l_1 = -\frac{\gamma-\alpha^3}{3\alpha s^2}, l_2 = -\frac{\beta_2\alpha-\beta_1}{3\alpha s^2}$. The kinetic energy is denoted by $\frac{P^2}{2}$, the potential energy by $-l_1\frac{\phi^2}{2} - l_2\frac{\phi^4}{4}$, and the total energy by g. By figuring out the structure $P = 0, l_1\phi + l_2\phi^3 = 0$, the points of equilibrium are $(0,0), (\sqrt{-\frac{l_1}{l_2}}), (-\sqrt{-\frac{l_1}{l_2}})$. The following is an expression for the Jacobian matrix for equation (7.1): $R(\phi, P) = \begin{vmatrix} 0 & 0 \\ l_1 + 3l_2\phi^2 & 0 \end{vmatrix} = -l_1 - 3l_2\phi^2$

A center point if $R(\phi, P) > 0$, a saddle point if $R(\phi, P) < 0$, and a cuspidal point if $R(\phi, P) = 0$ are the three possible appearances of the equilibrium point (ϕ, P). The following possible outcomes can arise from various parameter configurations:

Case 1: $l_1 < 0, l_2 > 0$

Using a selection of parameter settings such as $\gamma = 28, \alpha = 1, s = 1, \beta_1 = 2, \beta_2 = -1$. Three points of equilibrium can be found (0,0), (−3,0), (3,0). The saddle points are $(-3, 0)$ and (3, 0), whereas the origin (0, 0) acts as the center.

Case 2: $l_1 > 0, l_2 < 0$

Using a selection of parameter settings such as $\gamma = 13, \alpha = -1, s = 1, \beta_1 = 4, \beta_2 = -1$. Three points of equilibrium can be found (0,0), (−2,0), (2,0). The center points are $(-2, 0)$ and (2, 0), whereas the origin (0, 0) acts as the saddle.

Case 3: $l_1 < 0, l_2 < 0$

Using a selection of parameter settings such as $\gamma = 7, \alpha = 1, s = 1, \beta_1 = 6, \beta_2 = 12$. The point of equilibrium is (0,0). It can be seen clearly in the diagram that the origin (0,0) functions as the system's central point.

Case 4: $l_1 > 0, l_2 > 0$

Using a selection of parameter settings such as $\gamma = 11, \alpha = -1, s = 1, \beta_1 = -1, \beta_2 = -5$. The point of equilibrium is (0,0). It can be seen clearly in the diagram that the origin (0,0) functions as the system's saddle point. The dynamical system's phase portraits of these cases 1, 2, 3 and 4 are given in Figs. 11, 12, 13 and 14, respectively.

Chaotic behavior

Here we explore how perturbations influence the complexity of the dynamical system. Different representations are examined using 3D, 2D and time series phase planes are given in Figs. 15, 16 and 17. In order to gain insight into how this system behaves when elements are perturbed, we'll start by taking a closer look at the phase portrait picture.

$$\frac{d\phi}{d\xi} = P, \frac{dP}{d\xi} = l_1\phi + l_2\phi^3 + B\cos(\epsilon t). \tag{7.3}$$

Changes to the amplitude B and frequency ϵ of the disturbance in equation (7.3) are explored to understand what effect it's on the corresponding dynamical system. A fixed set of parameters allows us to investigate a range of conduct using both chaotic and quasi-periodic behaviors over different strengths and frequencies.

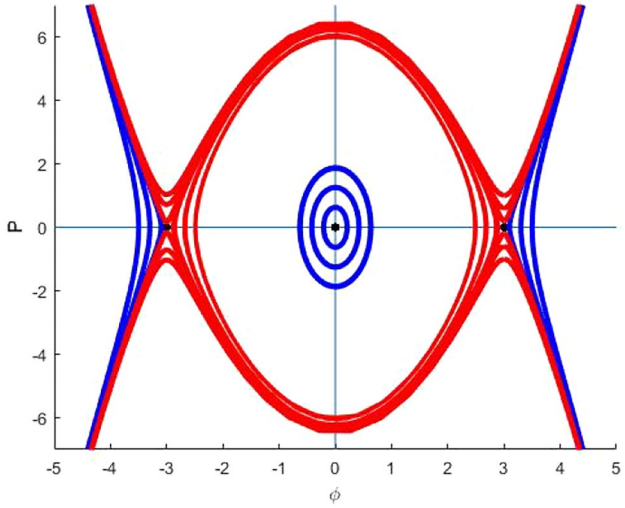

Fig. 11. The dynamical system's phase portraits when $l_1 < 0, l_2 > 0$.

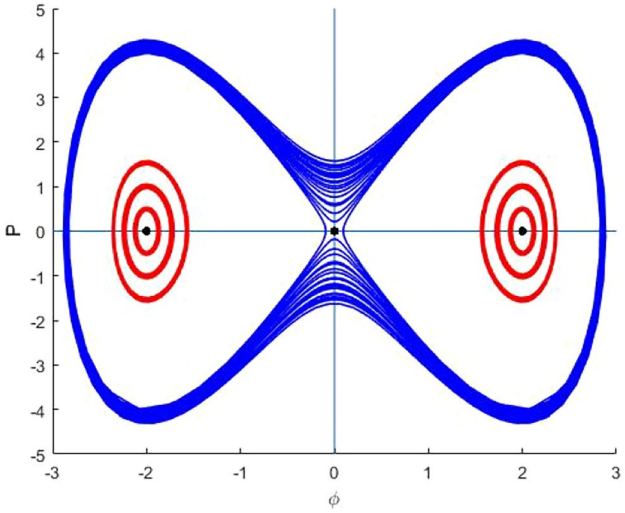

Fig. 12. The dynamical system's phase portraits when $l_1 > 0, l_2 < 0$.

Sensitivity analysis

Sensitivity analysis explores the ways in which changing small values of critical system parameters influences the system's response. Sensitivity analysis helps in decision-making and optimization by identifying the parameters that have the most effects on the system's results. The sensitivity analysis is important because it confirms that the obtained soliton solutions are robust against slight changes in the parameters. It demonstrates how the solitons maintain their stability in the face of perturbations, proving their physical significance and usefulness in systems like plasma wave propagation and optical fiber communications.. This part intends to study the effect of initial values on the disrupted structure equation (7.3) at different frequencies and intensities while maintaining the parameters $\gamma = 28, \alpha = 1, s = 1, \beta_1 = 2$ and $\beta_2 = -1$. Its graphical representation is given in Fig. 18.

Novelty and comparison

This section presents a brief comparison of our obtained exact soliton solutions in the form of kink, anti-kink, bell type, anti-bell type and periodic-solitons. kink and multi-soliton solutions, as well as other kinds of solitonic structures, in relation to the researchers' work[30,31] and brings the following to a close:

- Lu, D. *et.al.* applied the two analytical methods to find accurate solutions to the equation[30]. Seadawy *et.al* discussed the weakly nonlinear wave propagation of the generalized third-order NLSE and its applications[31].
- Compared to the previously published studies[30,31], we were able to find a variety of soliton solutions in a more generalized manner by employing the generalized auxiliary equation method and IMSSEM. The solutions have the shape of exponential, trigonometric and hyperbolic functions.

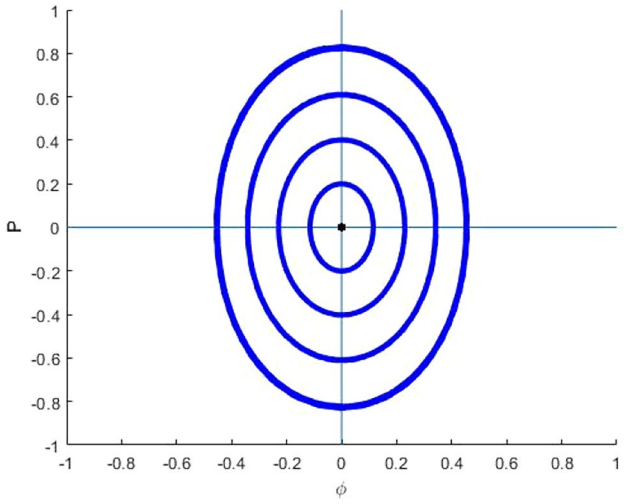

Fig. 13. The dynamical system's phase portraits when $l_1 < 0, l_2 < 0$.

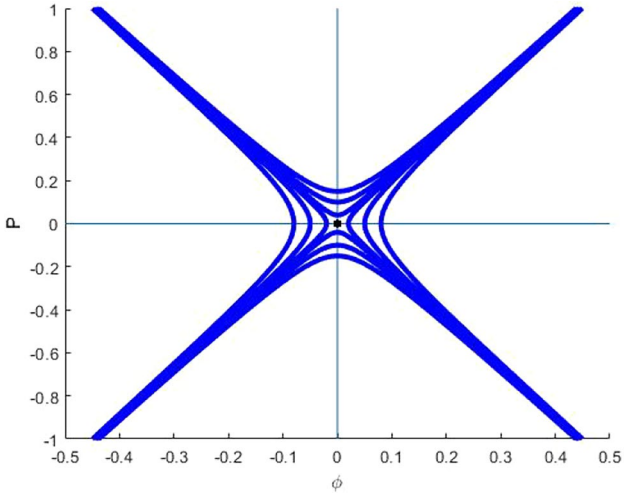

Fig. 14. The dynamical system's phase portraits when $l_1 > 0, l_2 > 0$.

- We used appropriate values for $s, p, \alpha, q_1, q_2, q, \beta_1, \beta_2$ and θ to illustrate the dynamics of solitary wave profiles of specific solitary solutions in 3D, 2D, and contour graphics.
- Additionally, the perturbed system's quasi-periodic solution is examined by adding definite forces to the model under consideration. Additionally, phase pictures are shown for the disturbed system that are not discussed in[30,31].
- Furthermore, sensitivity analysis and chaotic behavior for the perturbed system that are not displayed in[30,31] have been observed by us.

Conclusion

This work has investigated the soliton solutions of the generalized third-order NLSE. The generalized auxiliary equation method and improved modified Sardar-sub equation method have been effectively used to derive analytical solutions in a variety of formats, including periodic, bell or bright, kink soliton, anti-kink soliton and singular solitons. Some of the findings have been shown graphically. According to the findings, the generalized auxiliary equation method and IMSSEM have been proved more sophisticated, creative and effective methods for researching exact solutions of nonlinear equations in mathematical physics and engineering. The work offers new information on bifurcation structures, chaotic dynamics, and sensitivity behaviour of the model, unexplored systematically heretofore. The governing equation's related dynamical system have been derived first time using the Galilean transformation and the theory of the planar dynamical system was used to carry out the bifurcation analysis. The dynamical system with an external term analyzed for chaotic behaviors by representing a sequence of phase pictures in 2D, 3D and time series. Furthermore, sensitivity analysis has been performed on the dynamical system to make sure that minor adjustments to the initial conditions would not

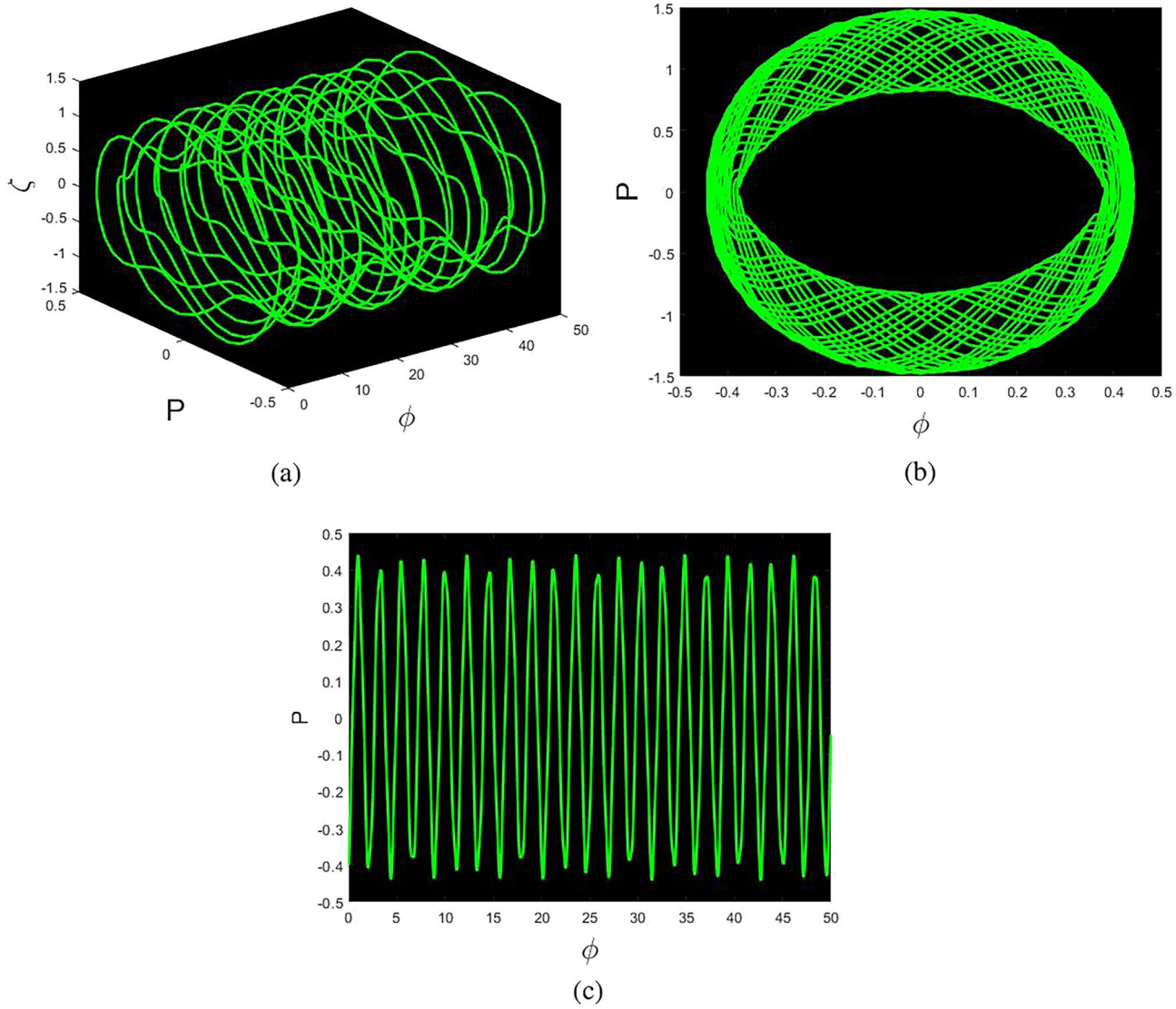

Fig. 15. Chaotic behavior of the equation (7.3) for $\gamma = 13, \alpha = -1, s = 1, \beta_1 = 4, \beta_2 = -1, B = 3, \epsilon = 10$..

have a major impact on the solutions. Future research can be extended to higher-order and stochastic models and their applications to optical and plasma systems.

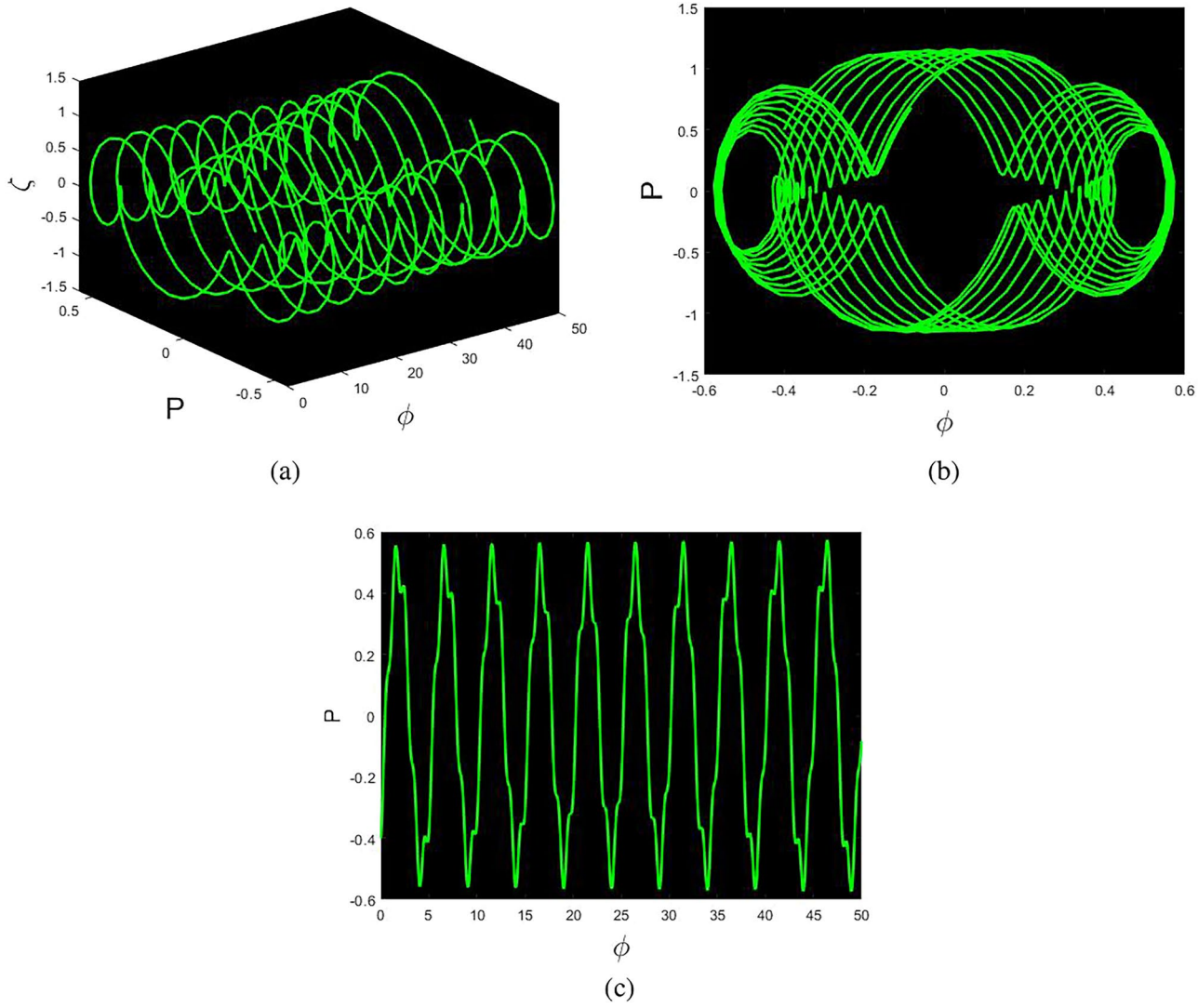

Fig. 16. Chaotic behavior of the equation (7.3) for $\gamma = 13, \alpha = -1, s = 1, \beta_1 = 4, \beta_2 = -1, B = 3, \epsilon = 2\pi$..

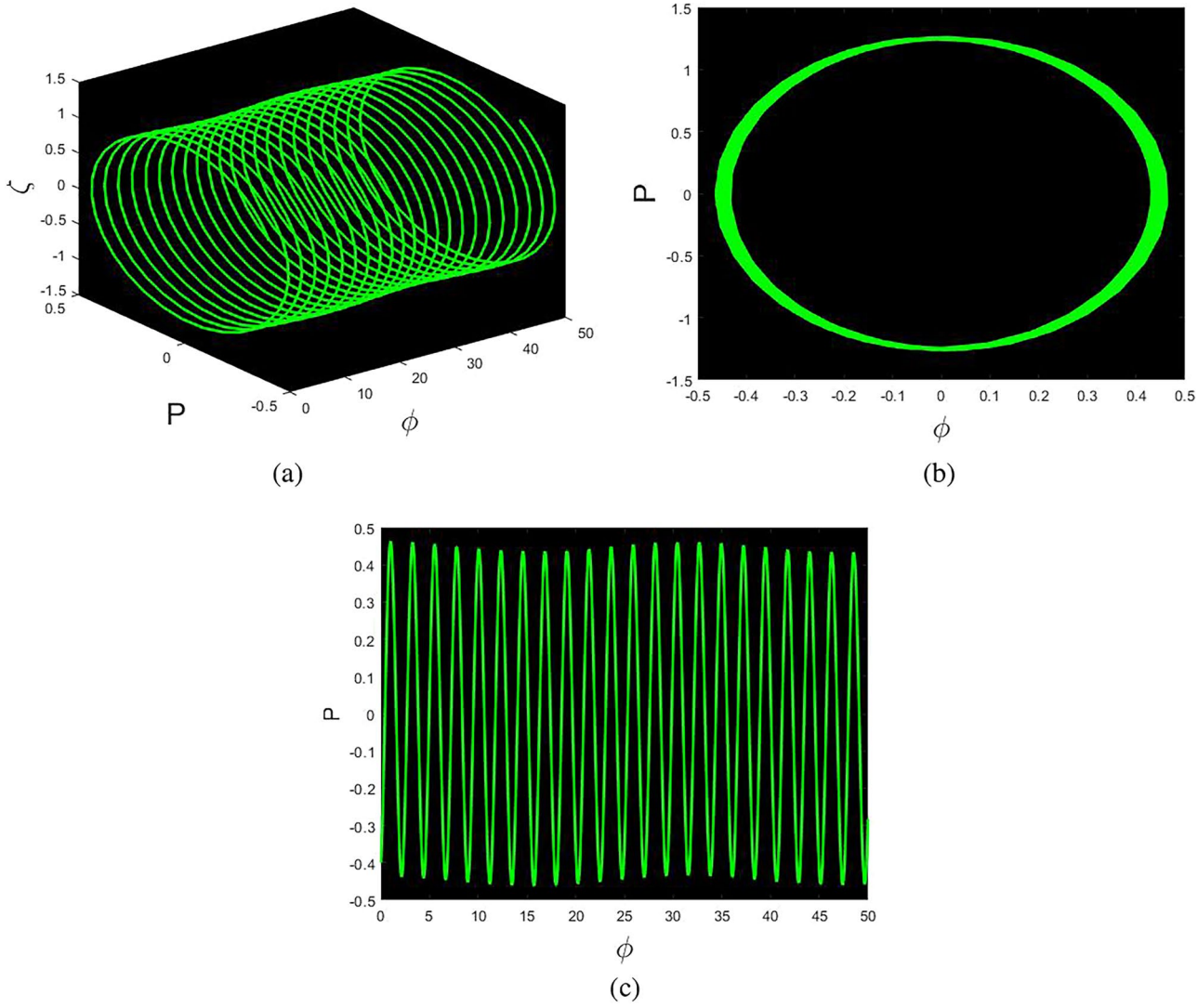

Fig. 17. Chaotic behavior of the equation (7.3) for $\gamma = 13, \alpha = -1, s = 1, \beta_1 = 4, \beta_2 = -1, B = 0.1, \epsilon = 0.2$..

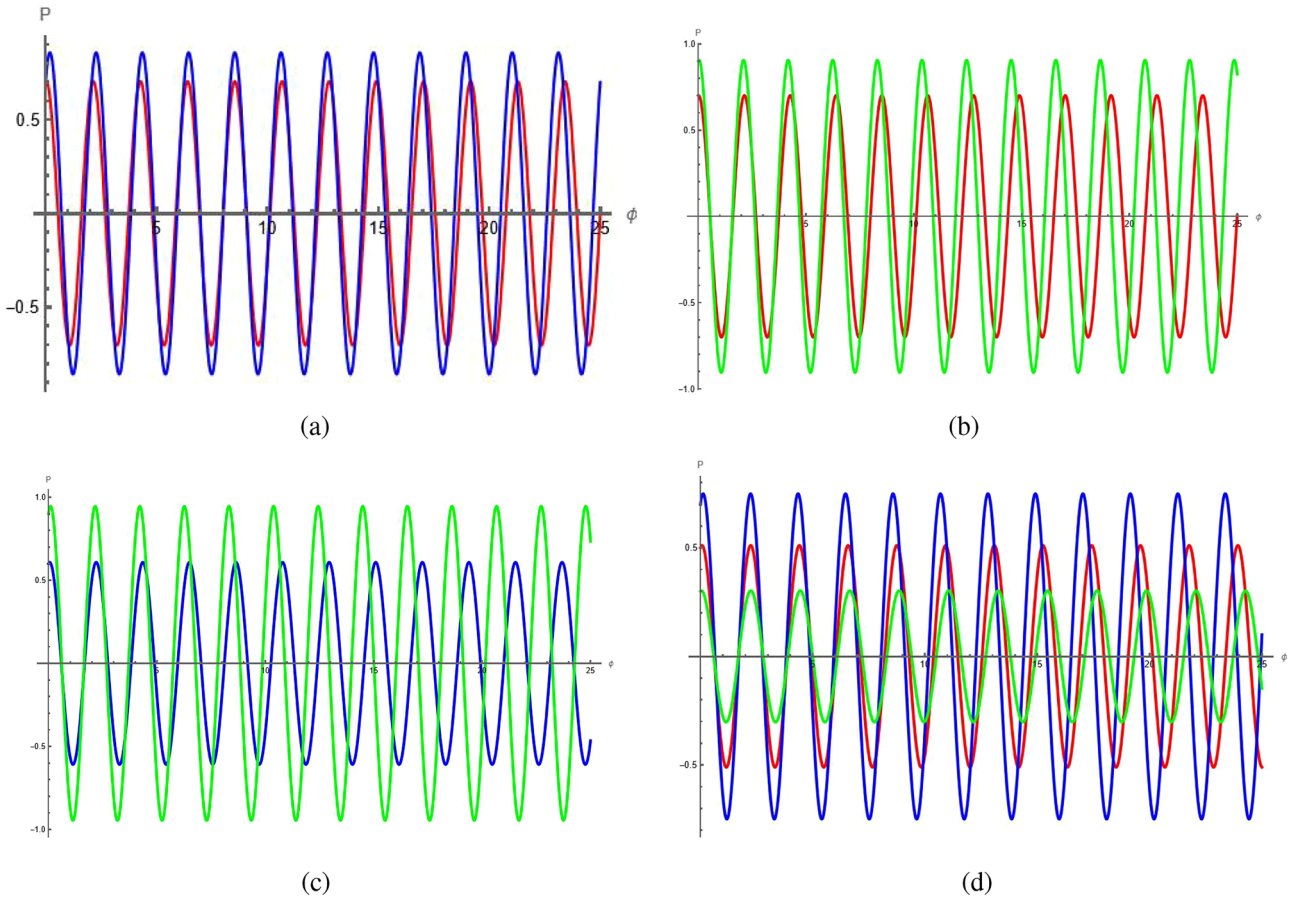

Fig. 18. Sensitivity analysis of the equation (7.3) for $\gamma = 13, \alpha = -1, s = 1, \beta_1 = 4, \beta_2 = -1$..

Data availability

Data sharing is not applicable to this article as no new data were created or analyzed in this study.

Received: 11 August 2025; Accepted: 27 January 2026
Published online: 03 February 2026

References

1. Zafar, A., Shakeel, M., Ali, A., Rezazadeh, H. & Bekir, A. Analytical study of complex Ginzburg-Landau equation arising in nonlinear optics. *Journal of Nonlinear Optical Physics & Materials* **32**(01), 2350010 (2023).
2. Kopçasız, B. Qualitative analysis and optical soliton solutions galore: scrutinizing the (2+ 1)-dimensional complex modified Korteweg-de Vries system. *Nonlinear Dynamics* **112**(23), 21321–21341 (2024).
3. Kopçasız, B. & Yaşar, E. M-truncated fractional form of the perturbed Chen-Lee-Liu equation: optical solitons, bifurcation, sensitivity analysis, and chaotic behaviors. *Optical and Quantum Electronics* **56**(7), 1202 (2024).
4. Kopçasız, B. Unveiling new exact solutions of the complex-coupled Kuralay system using the generalized Riccati equation mapping method. *Journal of Mathematical Sciences and Modelling* **7**(3), 146–156 (2024).
5. Kopçasız, B. & Yaşar, E. μn-Symmetries and μ-Conservation Laws for The Nonlinear Dispersive Modified Benjamin-Bona-Mahony Equation. *Journal of Mathematical Sciences and Modelling* **6**(3), 87–96 (2023).
6. Kopçasız, B. Exploration of soliton solutions and modulation instability analysis for cold bosonic atoms in a zig-zag optical lattice in quantum physics. *Nonlinear Dynamics*, 1-16 (2025).
7. Khater, M. M. & Owyed, S. Interplay between medium-induced nonlinearity and wave propagation characteristics: the nonlinear Tzitaeica-Dodd-Bullough model in nonlinear optics and electromagnetic waves. *Optical and Quantum Electronics* **57**(7), 407 (2025).
8. Khater, M. M. Nonlinear effects in quantum field theory: Applications of the Pochhammer-Chree equation. *Modern Physics Letters B* **39**(20), 2550070 (2025).
9. Khater, M. M. An integrated analytical-numerical framework for studying nonlinear PDEs: The GBF case study. *Modern Physics Letters B* **39**(20), 2550057 (2025).
10. Khater, M. M. Dynamics of propagation patterns: An analytical investigation into fractional systems. *Modern Physics Letters B* **39**(01), 2450397 (2025).
11. Khan, K. & Islam, M. S. The study of wave propagation for (2+ 1)-dimensional Bogoyavlenskii's breaking soliton system. *Zeitschrift für Naturforschung A* **80**(9), 879–888 (2025).
12. Khan, K., Koppelaar, H., Akbar, M. A. & Mohyud-Din, S. T. Analysis of travelling wave solutions of double dispersive sharma-Tasso-Olver equation. *Journal of Ocean Engineering and Science* **9**(5), 461–474 (2024).
13. Rahman, M. M., Islam, S. M., & Hoque, A. Investigations of soliton structures and dynamical behaviors of the Westervelt equation with two analytical techniques. *AIP Advances*, **15**(5), (2025).

14. Ozisik, M., Secer, A. & Bayram, M. On solitary wave solutions for the extended nonlinear Schrödinger equation via the modified F-expansion method. *Optical and Quantum Electronics* **55**(3), 215 (2023).
15. IIslam, S. R. Bifurcation analysis and exact wave solutions of the nano-ionic currents equation: Via two analytical techniques. *Results in Physics* **58**, 107536 (2024).
16. Shi, Q., Sun, Y. & Saanouni, T. On the growth of Sobolev norms for Hartree equation. *Journal of Evolution Equations* **25**(1), 13 (2025).
17. Huang, Z. Y., et al. Piecewise Calculation Scheme for the Unconditionally Stable Chebyshev Finite-Difference Time-Domain Method. *IEEE Transactions on Microwave Theory and Techniques* (2025).
18. Li, Y., Rui, Z. & Hu, B. Monotone iterative and quasilinearization method for a nonlinear integral impulsive differential equation. *AIMS MATHEMATICS* **10**(1), 21–37 (2025).
19. Ali, K. K., Alotaibi, M. F., Omri, M., Mehanna, M. S. & Abdel-Aty, A. H. Some Traveling Wave Solutions to the Fifth-Order Nonlinear Wave Equation Using Three Techniques: Bernoulli Sub-ODE, Modified Auxiliary Equation, and $\left(\frac{G'}{G}\right)$-Expansion Methods. *Journal of Mathematics* **2023**(1), 7063620 (2023).
20. Khan, M. I., Marwat, D. N. K., Sabi'u, J. & Inc, M. Exact solutions of Shynaray-IIA equation (S-IIAE) using the improved modified Sardar sub-equation method. *Optical and Quantum Electronics* **56**(3), 459 (2024).
21. Adem, A. R., Muatjetjeja, B. & Moretlo, T. S. An extended (2+ 1)-dimensional coupled burgers system in fluid mechanics: symmetry reductions; Kudryashov method; conservation laws. *International Journal of Theoretical Physics* **62**(2), 38 (2023).
22. Ibrahim, S., Ashir, A. M., Sabawi, Y. A. & Baleanu, D. Realization of optical solitons from nonlinear Schrödinger equation using modified Sardar sub-equation technique. *Optical and Quantum Electronics* **55**(7), 617 (2023).
23. Hosseini, K., Osman, M. S., Mirzazadeh, M. & Rabiei, F. Investigation of different wave structures to the generalized third-order nonlinear Scrödinger equation. *Optik* **206**, 164259 (2020).
24. Nasreen, N. et al. Stability analysis and dynamics of solitary wave solutions of the $(3+1)$-dimensional generalized shallow water wave equation using the Ricatti equation mapping method. *Results in Physics* **56**, 107226 (2024).
25. Hosseini, K., Hinçal, E. & Ilie, M. Bifurcation analysis, chaotic behaviors, sensitivity analysis, and soliton solutions of a generalized Schrödinger equation. *Nonlinear Dynamics* **111**(18), 17455–17462 (2023).
26. Li, P., Shi, S., Xu, C. & Rahman, M. U. Bifurcations, chaotic behavior, sensitivity analysis and new optical solitons solutions of Sasa-Satsuma equation. *Nonlinear Dynamics* **112**(9), 7405–7415 (2024).
27. Miah, M. M., Alsharif, F., Iqbal, M. A., Borhan, J. R. M. & Kanan, M. Chaotic Phenomena, Sensitivity Analysis, Bifurcation Analysis, and New Abundant Solitary Wave Structures of The Two Nonlinear Dynamical Models in Industrial Optimization. *Mathematics* **12**(13), 1959 (2024).
28. Shakeel, M., Liu, X., Mostafa, A. M., AlQahtani, N. F. & Alameri, A. Dynamic Solitary Wave Solutions Arising in Nonlinear Chains of Atoms Model. *Journal of Nonlinear Mathematical Physics* **31**(1), 70 (2024).
29. Muhammad, T. et al. Traveling wave solutions to the Boussinesq equation via Sardar sub-equation technique. *AIMS Math* **7**(6), 11134–49 (2022).
30. Lu, D., Seadawy, A. R., Wang, J., Arshad, M. & Farooq, U. Soliton solutions of the generalised third-order nonlinear Schrödinger equation by two mathematical methods and their stability. *Pramana* **93**, 1–9 (2019).
31. Seadawy, A. R., Arshad, M. & Lu, D. The weakly nonlinear wave propagation of the generalized third-order nonlinear Schrödinger equation and its applications. *Waves in Random and Complex Media* **32**(2), 819–831 (2022).

Acknowledgements
The authors would like to acknowledge the Deanship of Graduate Studies and Scientific Research, Taif University for funding this work.

Author contributions
SP: Methodology, Writing-original draft. MA: Supervision, Methodology, Writing-original draft. TZ: Supervision, Methodology, Writing-original draft. MNA: Formal Analysis, Writing-review & editing. MRA: Visualization, Writing-review & editing. MZY: Visualization, Writing-review & editing. AB: Funding acquisition, Writing-review & editing. All authors have read and agreed to publish the manuscript.

Funding
The author(s) received no external funding for this study.

Declarations

Competing interests
The authors declare no competing interests.

Additional information
Correspondence and requests for materials should be addressed to M.A. or A.B.

Reprints and permissions information is available at www.nature.com/reprints.

Publisher's note Springer Nature remains neutral with regard to jurisdictional claims in published maps and institutional affiliations.